Vol. 20, No. 2 (2021) 555-568
Revista Mexicana de Ingeniería Química

Effect of the adsorbent dose and initial contaminant concentration on the removal of Pb(II) in a solution using *Opuntia ficus* Indica shell

Efecto de la dosis de adsorbente y concentración inicial en la remoción de Pb(II) usando cáscara de *Opuntia ficus* Indica

C. Tejada-Tovar[1], H. Bonilla-Mancilla[2], A. Villabona-Ortíz[1], R. Ortega-Toro[3]* and J. Licares-Eguavil[4]

[1] *Universidad de Cartagena, Chemical Engineering Department, Avenida del Consulado Calle 30 No. 48 -152, Cartagena de Indias D.T. y C., Colombia.*
[2] *Universidad Nacional del Centro del Perú, Faculty of Forestry and Environmental Sciences. Mariscal Castilla 3909, Huancayo, Perú.*
[3] *Universidad de Cartagena, Food Engineering Department, Avenida del Consulado Calle 30 No. 48 - 152, Cartagena de Indias D.T. y C., Colombia.*
[4] *Universidad Nacional del Centro del Perú, Bachelor of Forest and Environmental Science of Forestry and Environmental Sciences. Mariscal Castilla 3909, Huancayo, Perú.*

Received: October 27, 2020; Accepted: December 19, 2020

Abstract

The effect of the adsorption capacity of Pb (II) on the shell of *Opuntia ficus* (tuna) was evaluated as a function of the adsorbent dose and initial contaminant concentration, in a batch system. The biomaterial was characterized by a nitrogen adsorption-desorption isotherm applying the BET equation, obtaining a surface area of 2.105 m^2/g. FTIR reported the presence of hydroxyl, carbonyl, alcohol and methoxy groups. SEM analysis showed that the surface of the tuna shell has the presence of mesopores and that after adsorption Pb (II) forms micro-complexes and precipitations in the exposed area due to ion exchange with the functional groups. EDS analysis after adsorption confirmed a high content of the metal in the tuna shell. 0.1 g of adsorbent and 90 mg/L were determined as the best conditions for adsorption, reporting a maximum removal capacity of 40.97 mg/g. The pseudo-second order and Elovich models adjusted the experimental data on kinetics; the isotherm was described by the Langmuir equation, determining that the process is controlled by chemisorption and occurs in a monolayer. The results found have potential application in the treatment of wastewater from some industries and mining.

Keywords: adsorption, bio-adsorbent, chemisorption, Langmuir model.

Resumen

Se evaluó el efecto de la capacidad de adsorción de Pb (II) sobre la cáscara de *Opuntia ficus* (tuna) en función de la dosis de adsorbente y la concentración inicial de contaminante, en un sistema por lotes. El biomaterial se caracterizó por una isoterma de adsorción-desorción de nitrógeno aplicando la ecuación BET, obteniendo una superficie de 2,105 m^2/g. El FTIR informó la presencia de grupos hidroxilo, carbonilo, alcohol y metoxi. El análisis SEM mostró que la superficie de la cáscara de tuna tiene presencia de mesoporos y que luego de la adsorción, el Pb (II) forma micro complejos y precipitaciones en el área expuesta debido al intercambio iónico con los grupos funcionales. El análisis de EDS después de la adsorción confirmó un alto contenido de metal en la concha de atún. Se determinaron 0,1 g de adsorbente y 90 mg/L como las mejores condiciones para la adsorción, reportando una capacidad máxima de remoción de 40,97 mg/g. Los modelos de pseudo segundo orden y Elovich ajustaron los datos experimentales en cinética; la isoterma fue descrita por la ecuación de Langmuir, determinando que el proceso está controlado por quimisorción y ocurre en una monocapa. Los resultados encontrados tienen potencial aplicación en el tratamiento de aguas residuales de algunas industrias y minería.

Palabras clave: adsorción, bio adsorbente, quimisorción, modelo de Langmuir.

* *Corresponding author. E-mail*: srortegap1@unicartagena.edu.co
https://doi.org/10.24275/rmiq/IA2134
ISSN:1665-2738, *issn-e*: 2395-8472

1 Introduction

The contamination of water sources by the discharge of effluents resulting from anthropogenic activities is one of the most significant environmental problems facing man today(Afroze & Sen, 2018). Among the most dangerous wastes are those containing heavy metals such as lead, nickel, chrome, cadmium, and mercury, among others, which harm aquatic life and human health, even at low concentrations, since they cause multiple pathologies and even death (Manirethan, Gupta, Balakrishnan, & Raval, 2019; Tran *et al.*, 2019). Lead is a metal highly resistant to the attack of corrosive acids such as sulphuric and hydrochloric, so it is widely used in different industrial sectors including mining, electroplating, battery, ceramics, electronics manufacturing, textiles, automotive, dyeing, among others (Allahdin, Mabingui, Wartel, & Boughriet, 2017; Basu, Guha, & Ray, 2017b; Rasmey, Aboseidah, & Youssef, 2018). Due to this, its annual consumption is around three millions of tons, of which 40% is used in the manufacture of electric accumulators and batteries, 12% in construction elements, 6% in the manufacture of cable sheaths, among other uses (Pan, Geng, Dong, Ali, & Xiao, 2019).

As a reactive metal, lead is rarely found in its elemental state. It is found in the form of salts, oxides, and organometallic compounds such as galena (PbS), lead ores associated with galena, complex sulphides such as anglesite ($PbSO_4$), cerussite ($PbCO_3$), and crocoite ($PbCrO_4$) (Morosanu, Teodosiu, Paduraru, Ibanescu, & Tofan, 2017). Due to its chemical load, it has been found that lead induces oxidative stress, by the excessive production of free radicals and causes damage to the cell membrane, through lipid peroxidation, since they are related by the thiol (SH), oxo (=O) and phosphate (PO_4^{3-}) groups found in some enzymes. Also, ligands and biomolecules of the organism affect the permeability of the organ membrane and the synthesis of haemoglobin (Boskabady *et al.*, 2018; Morosanu *et al.*, 2017; Candelaria; Tejada-Tovar, Bonilla-Mancilla, Del Pino-Moreyra, Ortega-Toro, & Villabona-Ortíz, 2020). Due to its high toxicity, different physicochemical methods have been tested in the removal of Pb (II) ions present in aqueous solution, including membrane processes, electrochemistry, ultrafiltration, reduction, photocatalysis, among others (Azimi, Azari, Rezakazemi, & Ansarpour, 2017; Bhanvase, Ugwekar, & Mankar, 2017). However, these technologies have drawbacks such as the use of reagents, high operating costs, and sludge generation. For this reason, the use of low-cost bio-adsorbents is an alternative to conventionally used technologies and includes the use of agricultural residues as bio-adsorbents which are efficient and reusable (Peng *et al.*, 2018; Raikar, Correa, & Ghorpade, 2015). Bio-adsorption takes advantage of the presence of functional groups in the structure of the residues such as carboxylic acids, alcohols, phenols, unsaturated hydrocarbons, and amines, due to their lignocellulosic origin (Obike, Igwe, Emeruwa, & Uwakwe, 2018; Villabona-Ortíz, Tejada-Tovar, & Ortega-Toro, 2020).

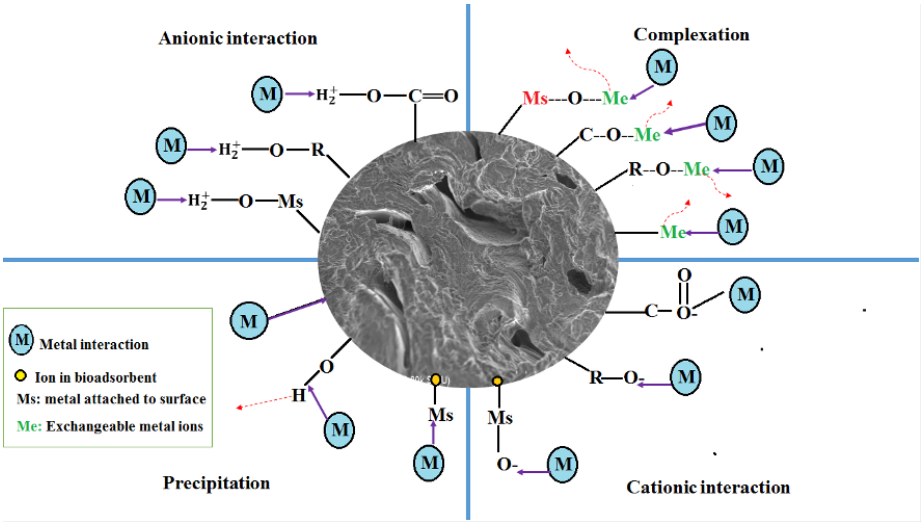

Fig. 1. Metal ion adsorption mechanism onto lignocellulosic biomass.

Table 1. Kinetic adsorption models.

Model	**Equation**	**Parameter**
Pseudo-first order	$q_t = q_e(1 - e^{-k_1 t}$	q_e (mg/g): Adsorption capacity at equilibrium q_t (mg/g): Adsorption capacity in a time t k_1 (min^{-1}): Lagergren's constant
Pseudo-Second order	$q_e = \frac{t}{\frac{1}{k_2 q_e^2} + \frac{t}{q_e}}$	k_1 (g^{-1} min^{-1}): Pseudo-second order constant
Elovich	$q_t = \frac{1}{\beta}\ln(\alpha\beta) + \frac{1}{\beta}\ln(t)$	α (mg g^{-1} min^{-1}): adsorption rate β (g/mg): Elovich's constant related to the extent of surface coverage and activation energy in chemisorption
Intraparticle diffusion	$q_t = k_3 t^{1/2}$	q_t (mg/g): amount of metal ion adsorbed per unit mass of adsorbent in a time t (min): time k_3 (mg/g.$min^{1/2}$): intraparticle diffusion constant
Second-order rate	$C_t = \frac{1}{k_2 t + \frac{1}{C_0}}$	C_t (mg/L): concentration of solute at time t C_o (mg/L): concentration of solute at equilibrium t (min): time k_2 (L/mg.min): second order rate constant
Liquid film diffusion	$q_t = q_e(1 - e^{-Rt})$ $R = \frac{3D_e^1}{r_o \Delta r_o k'}$	q_e (mg/g): Adsorption capacity at equilibrium q_t (mg/g): Adsorption capacity in a time t R (min^{-1}): liquid film diffusion constant D_e^1 (cm^2/min): effective liquid film diffusion coefficient r_o (cm): radius of adsorbent beads Δr_o (cm): thickness of liquid film k': equilibrium constant of adsorption
Double-exponential	$q_t = q_e - \frac{D_1}{m}e^{-K1t} - q_e - \frac{D_2}{m}e^{-K_2 t}$	D_1 (mmol/L): adsorption rate parameter of the rapid step K_1 (min^{-1}): adsorption diffusion parameters of the rapid step D_2 (mmol/L): adsorption rate parameter of the rapid step K_2 (min^{-1}): adsorption diffusion parameters of the rapid step m (g): adsorbent dose q_e (mmol/g): Adsorption capacity at equilibrium

Adapted from: Qiu *et al*., (2009).

The adsorption process can occur by different mechanisms of mass transfer of the adsorbate from the solution to the surface of the adsorbent and from there to its pores. Among these physicochemical transfer and reaction mechanisms are the anionic interaction, complexation, precipitation and cationic interaction (Figure 1) (Allahdin *et al*., 2017).

In order to interpret the mechanisms that control the adsorption processes, the kinetic study is carried out. The kinetics is initially controlled by the diffusion of the adsorbate from the solution to the exposed area of the adsorbent, the diffusion from the adsorbent surface into the pores. Also, the adsorption of metals by complexation, physicochemical adsorption, or ion exchange. (Basu, Guha, & Ray, 2017a). The

experimental kinetic data are adjusted to different theoretical models, and based on the adjustment of the parameters, it is possible to estimate the stages involved in the removal process. Table 1 lists some of the models most used in the literature (Qiu *et al*., 2009).

In the treatment of water contaminated with Pb (II), different residues of agricultural origin have been used as bio-adsorbents, among them: cocoa (Obike *et al*., 2018), rice (Saad, Amer, Tayeb, Nady, & Mohamed, 2020), lentils (Basu, Guha, & Ray, 2019), peas (ul Haq *et al*., 2017), plantain (Ibisi & Asoluka, 2018), dates seeds (Mahdi, Yu, & El Hanandeh, 2019), sorghum (Silas, 2017), agave fibres (Medellin-Castillo, 2017), yam shells and palm residues (Candelaria; Tejada-Tovar, Herrera-Barros, & Ruiz-Paternina, 2016). Finding those plant-based biomaterials is an excellent alternative for the removal of Pb(II) due to their chemical properties and physical characteristics (Amro, Abhary, Shaikh, & Ali, 2019). In this sense, the *Opuntia ficus* Indica, also known as tuna, is a wild plant with xerophilic nature, succulent, thorny, and arborescent representative of the regions of the arid or semi-arid climate, native to the American continent.

This plant has a significant amount of minerals such as Ca^{+2}, Mg^{+2}, Na^{+}, K^{+} and Fe^{+2}, and fibres like lignin, cellulose, hemicellulose, and pectin. It would be a suitable adsorbent of heavy metals since these components would propitiate the ionic exchange between the active centres and the Pb (II). Thus, the objective of the present study was to determine the effect of the adsorbent dose and the initial concentration on the removal of Pb (II) using the *Opuntia ficus* shell. The biomaterial was characterized by employing Scanning Electron Microscopy (SEM), Energy Dispersive X-Ray Spectroscopy (EDS), Fourier Transform Infrared Spectroscopy (FTIR), and the quantification of moisture, ash, and volatile content. The kinetics and adsorption isotherm were determined.

2 Materials and methods

2.1 Preparation and characterization of the bio-adsorbent

The tuna fruit was harvested from the Ayacucho region, washed with a sodium hypochlorite solution, dried at 60 °C for 72 hours to a constant mass, reduced in size, and sieved using the 1.0 mm mesh. The humidity, volatile matter, ash and fixed carbon content was determined following the standard ASTM D2974-14 (Cai *et al*., 2017). For this, the biomass was cut in sizes of 5 to 7 mm and placed in a muffle at 700 °C for 1h. Then, 5 g of dry material (M1) was taken and placed at 110 °C for another hour and then weighed (M2). The samples were placed at 700 °C; one sample was left for 15 minutes to determine its dry weight and the amount of volatile material (M3) and the other one for 1 hour to determine the ash content (M4). The percentages of moisture, volatile material and ash were determined using the following equations 1, 2, 3 and 4.

$$\%\text{Humidity} = \left(\frac{M_1 - M_2}{M_1}\right) \times 100 \tag{1}$$

$$\%\text{Volatile} = \left(\frac{M_2 - M_3}{M_1}\right) \times 100 \tag{2}$$

$$\%\text{Ashes} = \left(\frac{M_4}{M_1}\right) \times 100 \tag{3}$$

$$\%\text{Humidity} + \%\text{Volatile} + \%\text{Ashes} + \%\text{fixed carbon} = 100\% \tag{4}$$

The bio-adsorbent was characterized by Fourier Transform Infrared Spectroscopy analysis using an FTIR spectrophotometer (Perkin, Elmer FT-IR MIR/NIR Frontier) to identify the functional groups involved in the Pb (II) adsorption process (Azimi *et al*., 2017). Scanning Electronic Microscopy (SEM Hitachi SU8230) and X-Ray Emission Spectroscopy (EDS AnalytJena Nova Pro 400) using gold as the conducting agent to study the morphology and interaction mechanisms of Pb (II) with the active centres located on the surface of the bio-adsorbent(Peng *et al*., 2018). Also, nitrogen adsorption curve analysis was done by the Brunauer-Emmett-Teller (BET) method at -196.15 °C with a relative pressure range (P_0) between 0.005 and 1 to calculate the contact surface area, porosity and type of pores present on the prickly pear surface (Candelaria; Tejada-Tovar *et al*., 2020).

2.2 Adsorption test

Pb (II) removal tests were performed in triplicate using 50 mL of solution, at 150 rpm, 18 °C, pH 5, and following a 2k factorial experimental design with three levels of variation for two factors:

adsorbent dose (0.1, 0.2, 0.3 g) and initial contaminant concentration (30, 60, 90 ppm). The synthetic solution was prepared using Analytical Grade Lead Nitrate ($Pb(NO_3)_2$) 99.5% pure Merk Millipore brand. The pH was adjusted using Sodium Hydroxide (NaOH) and analytical grade Nitric Acid (HNO_3) LOBA-Chemie brand to 99.0%. The final concentration of metal remaining in the solution was determined by atomic absorption at 217 nm (Osińska, 2017).

2.3 Kinetics and adsorption isotherm

The kinetic and equilibrium study was performed at the best conditions of adsorbent dose and initial concentration of contaminants found in the adsorption tests, to establish the saturation time of the biomass and the adsorbent removal capacity when equilibrium is reached. For the kinetics, aliquots were taken every 10 min during the first hour. This fact is due to the adsorption process occurs rapidly at the beginning because the bio-adsorbent is unsaturated. Subsequently, samples were taken every 20 min until completing 2h. The experimental data were adjusted to the kinetic models (pseudo-first order, pseudo-second order, Elovich, and Intraparticle Diffusion) using the OriginPro 8® software, calculating the adjustment parameters and the correlation coefficient (R^2). The isotherms were performed during 24 h varying the initial concentration of contaminant (50, 80, 90, 100, 150, and 200 ppm) at 150 rpm, 100 mL, and 18 °C. The Langmuir, Freundlich, and Dubinin-Radushkevich models were selected to adjust the experimental data(Yu & He, 2018).

3 Results and discussion

3.1 Characterization of the bio-adsorbent

Tuna is a fruit belonging to the cactus family with a characteristic taste and many attributes and is mostly consumed fresh. The humidity content of 80.42% was determined, which is characteristic of this plant because it is a cactus with high water content. However, its life span is long, with a prolonged time of ageing (Kan, Strezov, & Evans, 2016). The ash content of 1.05% indicates that the biomass does not contain inorganic compounds such as heavy metals and is due to the presence of silica, aluminium, iron, calcium, titanium, magnesium, sodium, and potassium oxides. The volatile content of 12.77% implies a higher amount of bio-oil production through pyrolysis23. The fixed carbon content in tuna is 5.76%, due to the high content of carbohydrate polymers present in the structure of the biomaterial due to its lignocellulosic nature (Singh, Mahanta, & Bora, 2017).

The Fourier Transform Infrared Spectroscopy (FTIR) allowed to know the surface chemistry of the biomass and to obtain information about the functional groups present on the surface of the biomass. This information is decisive in the process of Pb (II) adsorption and provides hydrophilic properties to the biomass since they increase the specific ion-active centre interaction (Saravanan, Kumar, Carolin, & Sivanesan, 2017).

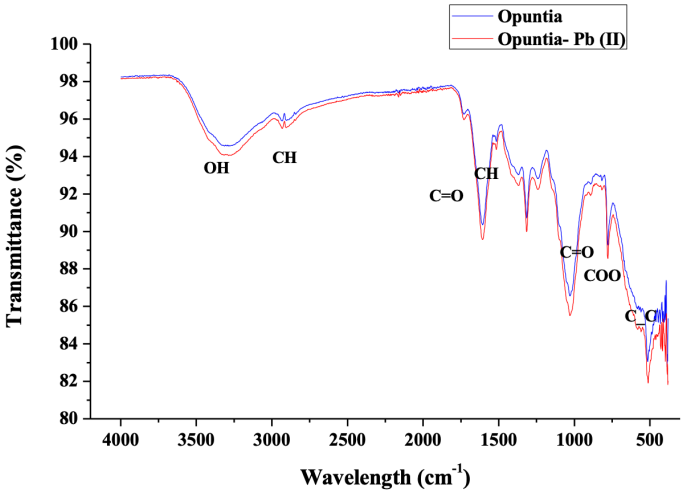

Fig. 2. FTIR spectrum of tuna before and after Pb (II) adsorption.

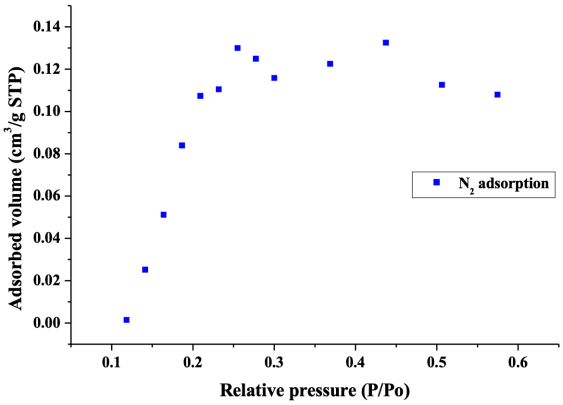

Fig. 3. N_2 adsorption isotherm.

The IR spectrum is shown in Figure 2, a prominent peak of 3438 cm^{-1} was found indicating the stretching of the hydroxyl group, 3273 - 3504.4 cm^{-1} belong to the stretching of the cellulose, hemicellulose, lignin, water (Rinaldi, Yasdi, & Hutagalung, 2018). The stretch around 1735.8 cm^{-1} corresponds to the carbonyl group C=O, which represents the active sites of the carboxyl group of pectin, hemicellulose, and lignin (Joshi, Singh, & Rajput, 2018). The peak at 1407.9 cm^{-1} shows the presence of C-H groups, representing aliphatic and aromatic groups such as methyl and methoxy groups, and the band from 1359.7 cm^{-1} to 1056.9 cm^{-1} corresponds to the C-O group of alcohols, esters, and aldehydes (Zhou *et al*., 2017). The absorption peaks in the region of 3540 to 3200 cm^{-1} are due to the extension of the OH-NH (Gola, Malik, Namburath, & Ahammad, 2018). After Pb (II) adsorption, the bands present a slight stretching due to the entrance of the metal, a masking of the carboxylic and hydroxyl groups were observed in the presence of Pb (II) (Abdolali *et al*., 2017).

The porosity of the prepared adsorbent is an important variable that affects the performance of the adsorption process. Nitrogen adsorption measurements for tuna are presented in Figure 3 and represent a picture on the readily available surface area. According to the shape of the isotherm, it is identified as type IV, according to the IUPAC classification. After filling the micropores, multilayer adsorption occurs, which is expected in biological samples that have micro and mesopores. The pore size distribution, another essential feature, exemplifies the physical heterogeneity of the adsorbing surface (El-Azazy *et al*., 2019). The surface area of biomass by the BET model was 2.1050 m^2/g, with pore volume of 0.08179 cm^3/g. Pore volume was low, this was attributed to the structure of lignocellulosic carbohydrates polymers, such as cellulose and lignin, which are characterized by reduced quantities of pores and blocked pores (Candelaria Tejada-Tovar, Gonzalez-Delgado, & Villabona-Ortiz, 2019).

The surface morphology before and after the deposition of lead ions on tuna surface was determined by SEM analysis. The micrographs are shown in Figure 4. The surface of the *Opuntia ficus* shell has the presence of pores that appear as dark cavities, which infers the ability of BPP to absorb metal ions (Feizi & Jalali, 2015). After the Pb (II) bio-adsorption, the deposition of the ions is observed on the irregular adsorbent surface, as evidenced by the bright precipitations of more than 3μm in Figure 3b, which suggests that the adsorption process occurs in monolayer (Kaur, Kumari, & Sharma, 2020).

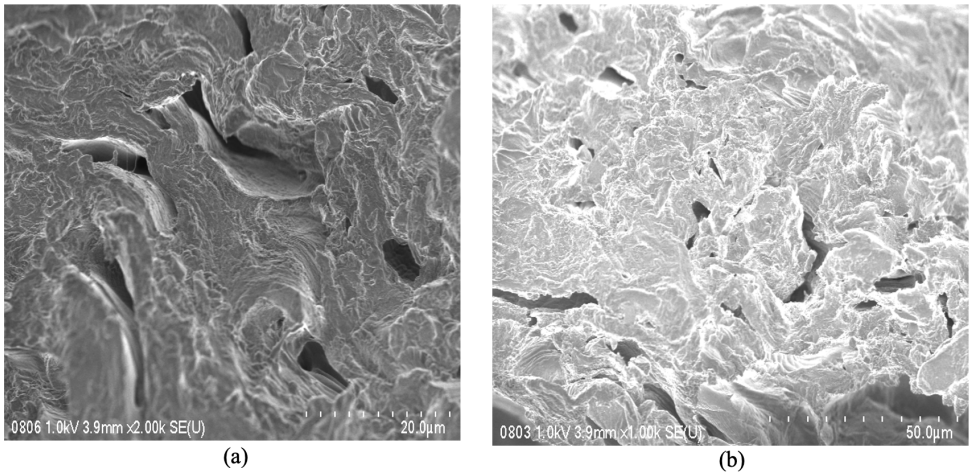

(a) (b)

Fig. 4. SEM micrographs of tuna (a) before and (b) after Pb (II) adsorption.

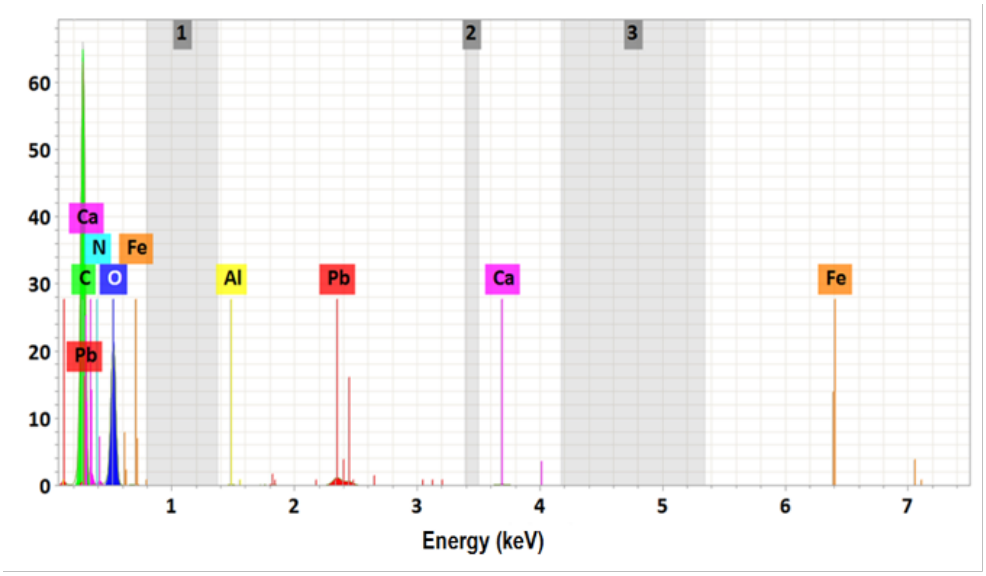

Fig. 5. EDS spectrum of tuna after removal of Pb (II).

Figure 5 shows the EDS spectrum for tuna after Pb (II) removal; carbon was identified as the element with the highest proportion (41.61%), followed by oxygen (39.01%). The presence of these two elements is due to the content of lignin, hemicellulose, cellulose and pectin in its structure, which makes it a suitable adsorbent material as confirmed by the presence of Pb with 12.53%w in the characteristic peak of Pb in 2.3 keV. Also, the presence of Fe (0.75%w), Al (0.16%w), and Ca (5.07%w) were shown. The change in the structure of the material after Pb(II) adsorption (Figure 2) and the appearance of precipitated particles on the surface (Figure 4b) could be attributed to the mechanism of ion binding in the active centres. This process is controlled by the formation of micro-complexes and precipitates on the tuna surface. Pb(II) is retained at the contact sites by ion exchange between the metal and the active centres of the adsorbent (Malik, Dahiya, & lata, 2017).

3.2 Removal of Pb(II)

The adsorbent dose is a determining variable in the adsorption processes since it has an intrinsic relationship with the availability of active sites in the adsorbent (Amro *et al*., 2019). On the other hand, the initial concentration is one of the driving forces of the mass transfer and intra-particle diffusion that occur during adsorption, since they establish the availability of metal ions (Malik *et al*., 2017). Figure 6 shows the average results of these two variables concerning the adsorption capacity of Pb (II) on the shell of tuna, finding the highest at 0.1 g of adsorbent and initial concentration of 90 mg/L. Table 2 shows the results of the analysis of variance with 95% confidence for the adsorption capacity with a 95% confidence level. The two variables evaluated have a significant effect on the process of Pb(II) removal.

Table 2. ANOVA of Pb (II) adsorption capacity on tuna.

Fuente	**Suma de Cuadrados**	**Gl Razón-F**	**P-Value**	
A:Adsorbent dose	1623.27	1	1730.15	0.0000
B:Initial concentration	1142.97	1	1218.22	0.0000
AA	129.896	1	138.45	0.0000
AB	236.071	1	251.61	0.0000
BB	0.112044	1	0.12	0.7335
bloques	0.169896	2	0.09	0.9138
Error total	17.8264	19		
Total (corr.)	3150.32	26		

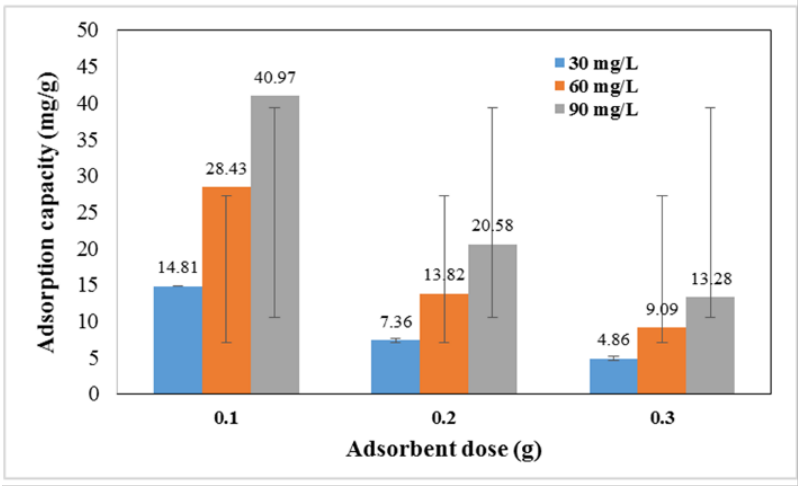

Fig. 6. Adsorption capacity of Pb (II) on tuna shells at different doses of adsorbent and initial concentration.

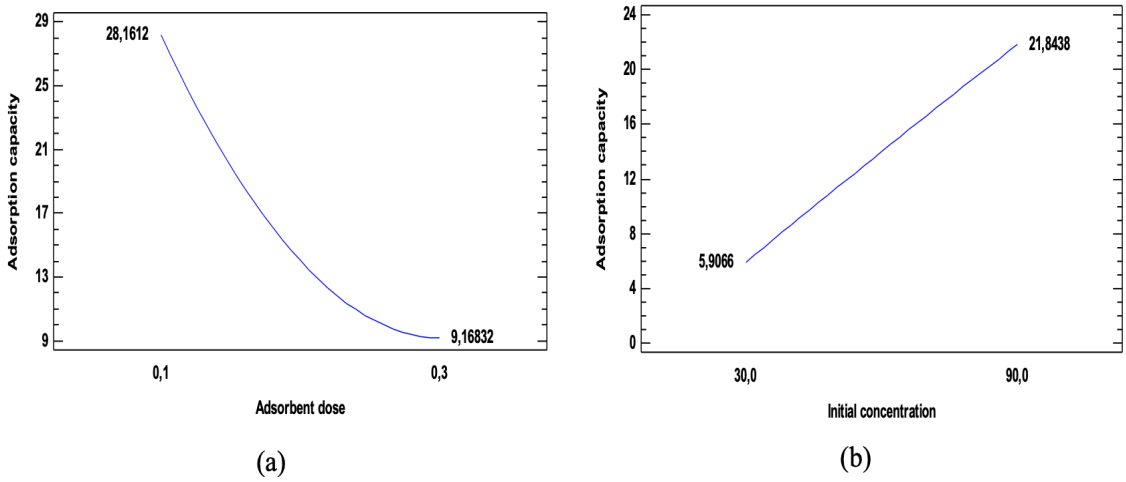

Fig. 7. Effect of the adsorbent dose (a) and initial concentration (b) on the adsorption capacity of Pb (II).

Table 3. Adjustment parameters of isothermal models for Pb (II) adsorption equilibrium on tuna.

Model	Parameters	Lead
Langmuir	q_{max} (mg/g)	58.8432
	b (L/mg)	0.6088
	R^2	0.9851
Freundlich	K_f (L/g)	30.6593
	1/n	0.1448
	n	6.0908
	R^2	0.9679
Dubinin-Radushkevic	q_{DR} (mg/g)	51.6427
	k_{DR} (mol^2/kJ^2)	2.4374E-7
	E (kJ/mol)	45.2920
	R^2	0.9046

Figure 7a reflects the adverse effect of increasing the amount of adsorbent on the adsorption capacity of Pb(II), which is attributed to a higher dose of adsorbent providing more active adsorption sites which even after the removal process remain unsaturated (Osińska, 2017). According to the ANOVA (Table 2), the interactions at initial concentration-dose of adsorbent also have a significant effect on the adsorption capacity of the bio-adsorbent. This fact could be promoted by a decrease in the total contact surface area. The length increase of the diffusion path as a result of the overlapping or aggregation of adsorption sites provokes a decrease in the removal capacity of the tuna (Akpomie, Eluke, Ajiwe, & Alisa, 2018). Although the number of adsorption sites per unit mass of an

adsorbent must be constant independent of the total adsorbent mass, increasing the mass of the adsorbent in a fixed volume of the solution decreases the effective surface area. As a result, available sites decrease promotes a reduction of metal adsorbed in the adsorbent (Silas, 2017).

On the other hand, the adsorption capacity shows a linear increase with the increase of the initial concentration of Pb (II), which is due to the expansion of the adsorption driving forces so that mass transfer and diffusion from the solution sine to the exposed surface of the adsorbent occurs (Feizi & Jalali, 2015). An increase in the initial concentration improves the interaction between the metal ions and the active sites as a result of the increased collision. This event increases the ions fixed on the surface of the adsorbent (Silas, 2017).

3.3 Adsorption kinetics

Adsorption kinetics describes the trapping rate of the adsorbate as well as the lifetime of the adsorbent before saturation (Kaur *et al*., 2020). The fit of Pb (II) adsorption kinetics to the pseudo-first order, pseudo-second order, Elovich and intraparticle diffusion models is shown in Figure 8. The setting parameters are summarized in Table 3. Based on Figure 8, a fast adsorption rate is observed during the first 40 min, reaching equilibrium at about 80 min, which implies a high selectivity of the active sites by the metal ions (Gorimbo, Taenzana, Muleja, Kuvarega, & Jewell, 2018; Taşar, Kaya, & Ozer, 2014).

Adsorption can occur through different types of transfer mechanisms from the adsorbate to the adsorbent. The kinetics is mainly controlled by several factors such as diffusion of the adsorbate from the solution to the adsorbent exposed area (mass diffusion), diffusion from the adsorbent surface into the pores, and adsorption of metals by complexation, physicochemical adsorption, or ion exchange. This process occurs in sequential stages/steps (Huang *et al*., 2017; Taşar *et al*., 2014). From the parameters in Table 3 and Figure 8, it can be said that the pseudo-second order and Elovich models describe the adsorption mechanism of the process, which suggests that the limiting step of Pb (II) adsorption on tuna is chemical adsorption (Amro *et al*., 2019), as shown in Figure 1. From the fit to the intraparticle Diffusion model and the value of the adsorption speed constant, it can be said that the adsorption is controlled in its initial stages by the diffusion.

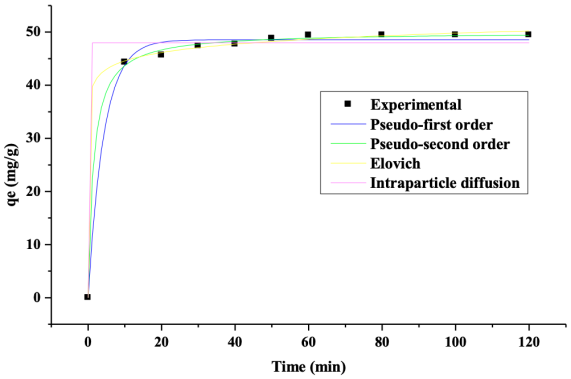

Fig. 8. Non-linear adjustment of experimental data on the adsorption kinetics of Pb (II) on tuna.

This process is carried out through the liquid to the adsorbent exposed surface, then diffusing into the pores, which would explain the fast speed of adsorption during the first minutes of the kinetics (Dai *et al*., 2018).

3.4 Adsorption isotherm

Adsorption equilibrium isotherms are used to relate the concentration of adsorbate in solution and the amount in the equilibrium adsorbent, as they provide information on the adsorption mechanism, surface properties and affinity of the adsorbents, which helps to determine the applicability of the process as a unitary operation. Therefore, it is essential to establish the most appropriate correlation of the equilibrium curves to optimize the conditions for designing the adsorption system (Silas, 2017). Figure 9 shows the fit of the experimental data to the Langmuir, Freundlich, and Dubninin-Radushkevich models.

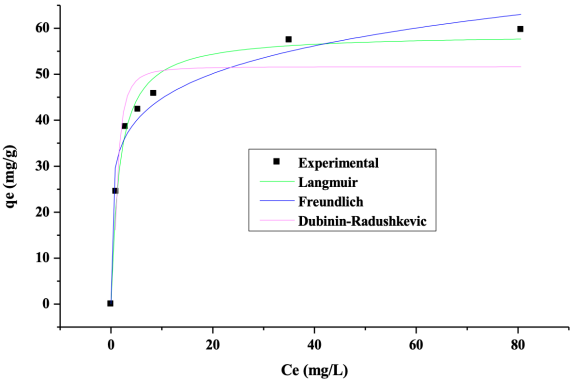

Fig. 9. Non-linear adjustment of the Pb (II) adsorption isotherm on tuna.

According to Figure 9 and the adjustment parameters (Table 4), it is established that the model which best describes the adsorption equilibrium is Langmuir, with a qmax of 58.54 mg/g close to the experimental one. Assuming the process occurs with a uniform distribution in the form of a monolayer on the exposed surface of the adsorbent as shown in Figure 4b, caused by the diffusive phenomena which control initial stages of Pb (II) removal (Asuquo, Martin, Nzerem, Siperstein, & Fan, 2017). On the other hand, according to the satisfactory fit of Freundlich's model and the value of n>1 is confirmed the heterogeneity of tuna shell, according to Figure 1, and the high value of K_f implies a high rate of metal adsorption in the contact area of the adsorbent (El-Moselhy, Abdel Azzem, Amer, & Al-Prol, 2017; Kebede, Dube, Mhuka, & Nindi, 2019).

Conclusions

(i) From the Pb (II) adsorption tests on tuna shells, the maximum adsorption capacity of 40.97 mg/g was reached using 0.1 g of adsorbent and 90 mg/L of initial concentration. (ii) Both variables under study presenting a significant effect on the process with removal efficiencies above 87% in all cases. (iii) The chemical-proximal analysis showed that the biomaterial does not have inorganic compounds of high molecular weight, with a long-life span and a high content of hydrocarbon compounds in its structure. (iv) A surface area of 2.105 m^2/g was obtained for the isotherm of nitrogen adsorption-desorption for the tuna shell.

The SEM-EDS analysis suggests that the mechanisms of adsorption in the bio-adsorbent are given by the formation of micro-complexes and precipitation in the exposed contact area of the tuna, through cation exchange with the -COOH, -OH, -R-OH groups confirmed in the FTIR. (v) A rapid rate of adsorption during kinetics was presented, reaching equilibrium at 80 min, with the PSO and Elovich models being the best suited to the experimental data suggesting that the limiting step is the chemical reaction. (vi) Adsorption isotherms were described by Langmuir's model, indicating the metal is adsorbed on the surface of the metal in a monolayer. (vii) Tuna shell is recommended as an effective bio-adsorbent for the removal of the metal under study; the importance of this work lies in the successful use of agro-industrial waste in the removal of heavy metals from aqueous solutions. These results have potential application in the treatment of industrial and mining wastewater.

Acknowledgements

The authors thank the collaborators of the Universidad Nacional del Centro de Perú and Universidad de Cartagena (Colombia) for the support in the development of this work regarding laboratory, software use, and time for their researchers.

Nomenclature

M1	Dry material mass
M2	Mass of material after 1 hour of drying at 110 ºC
M3	Mass of material after 15 min of drying at 700 ºC
M4	Mass of material after 1 hour of drying at 700 ºC
rpm	Revolutions per minute

References

Abdolali, A., Ngo, H. H., Guo, W., Zhou, J. L., Zhang, J., Liang, S., ...Liu, Y. (2017). Application of a breakthrough biosorbent for removing heavy metals from synthetic and real wastewaters in a lab-scale continuous fixed-bed column. *Bioresource Technology*. https://doi.org/10.1016/j.biortech.2017.01.016

Afroze, S., & Sen, T. K. (2018). A Review on Heavy Metal Ions and Dye Adsorption from Water by Agricultural Solid Waste Adsorbents. *Water, Air & Soil Pollution 229*, 225. https://doi.org/10.1007/s11270-018-3869-z

Akpomie, K. G., Eluke, L. O., Ajiwe, V. I. E., & Alisa, C. O. (2018). Attenuation kinetics and desorption performance of artocarpus altilis seed husk for Co(II), Pb(II) And Zn(II) Ions. *Iranian Journal of Chemistry and Chemical Engineering 37*, 171-186.

Allahdin, O., Mabingui, J., Wartel, M., & Boughriet, A. (2017). Removal of Pb2+ ions from aqueous solutions by fixed-BED column using a modified brick: (Micro)structural, electrokinetic and mechanistic aspects. *Applied Clay Science,*

148, 56-67. https://doi.org/10.1016/j.clay.2017.08.002

Amro, A. N., Abhary, M. K., Shaikh, M. M., & Ali, S. (2019). Removal of lead and cadmium ions from aqueous solution by adsorption on a low-cost Phragmites biomass. *Processes 7*, 406. https://doi.org/10.3390/pr7070406

Asuquo, E., Martin, A., Nzerem, P., Siperstein, F., & Fan, X. (2017). Adsorption of Cd(II) and Pb(II) ions from aqueous solutions using mesoporous activated carbon adsorbent: Equilibrium, kinetics and characterisation studies. *Journal of Environmental Chemical Engineering 5*, 679-698. https://doi.org/10.1016/j.jece.2016.12.043

Azimi, A., Azari, A., Rezakazemi, M., & Ansarpour, M. (2017). Removal of heavy metals from industrial wastewaters: A Review. *ChemBioEng Reviews 4*, 37-59. https://doi.org/10.1002/cben.201600010

Basu, M., Guha, A. K., & Ray, L. (2017a). Adsorption behavior of cadmium on husk of lentil. *Process Safety and Environmental Protection 106*, 11-22. https://doi.org/10.1016/j.psep.2016.11.025

Basu, M., Guha, A. K., & Ray, L. (2017b). Adsorption of lead on cucumber peel. *Journal of Cleaner Production 151*, 603-615. https://doi.org/10.1016/j.jclepro.2017.03.028

Basu, M., Guha, A. K., & Ray, L. (2019). Adsorption of lead on lentil husk in fixed bed column bioreactor. *Bioresource Technology 283*, 86-95. https://doi.org/10.1016/j.biortech.2019.02.133

Bhanvase, B. A., Ugwekar, R. P., & Mankar, R. B. (2017). *Novel Water Treatment and Separation Methods: Simulation of Chemical Processes*. Waretown: Apple Academic Press, INC.

Boskabady, M., Marefati, N., Farkhondeh, T., Shakeri, F., Farshbaf, A., & Boskabady, M. H. (2018). The effect of environmental lead exposure on human health and the contribution of inflammatory mechanisms, a review. *Environment International 120*, 404-420. https://doi.org/10.1016/j.envint.2018.08.013

Cai, J., He, Y., Yu, X., Banks, S. W., Yang, Y., Zhang, X., ... Bridgwater, A. V. (2017). Review of physicochemical properties and analytical characterization of lignocellulosic biomass. *Renewable and Sustainable Energy Reviews 76*, 309-322. https://doi.org/10.1016/j.rser.2017.03.072

Dai, Y., Sun, Q., Wang, W., Lu, L., Liu, M., Li, J., ... Zhang, Y. (2018). Utilizations of agricultural waste as adsorbent for the removal of contaminants: A review. *Chemosphere 211*, 235-253. https://doi.org/10.1016/j.chemosphere.2018.06.179

El-Azazy, M., El-Shafie, A. S., Issa, A. A., Al-Sulaiti, M., Al-Yafie, J., Shomar, B., & Al-Saad, K. (2019). Potato peels as an adsorbent for heavy metals from aqueous solutions: eco-structuring of a green adsorbent operating plackett-burman design. *Journal of Chemistry 2019*. https://doi.org/10.1155/2019/4926240

El-Moselhy, K., Abdel Azzem, M., Amer, A., & Al-Prol, A. (2017). Adsorption of Cu(II) and Cd(II) from aqueous solution by using rice husk adsorbent. *Physical Chemistry: An Indian Journal 12*, 109-122.

Feizi, M., & Jalali, M. (2015). Removal of heavy metals from aqueous solutions using sunflower, potato, canola and walnut shell residues. *Journal of the Taiwan Institute of Chemical Engineers 54*, 125-136. https://doi.org/10.1016/j.jtice.2015.03.027

Gola, D., Malik, A., Namburath, M., & Ahammad, S. Z. (2018). Removal of industrial dyes and heavy metals by Beauveria bassiana: FTIR, SEM, TEM and AFM investigations with Pb(II). *Environmental Science and Pollution Research 25*, 20486-20496. https://doi.org/10.1007/s11356-017-0246-1

Gorimbo, J., Taenzana, B., Muleja, A. A., Kuvarega, A. T., & Jewell, L. L. (2018). Adsorption of cadmium, nickel and lead ions: equilibrium, kinetic and selectivity studies on modified clinoptilolites from the USA and RSA. *Environmental Science and Pollution Research 25*, 30962-30978. https://doi.org/10.1007/s11356-018-2992-0

Huang, X., Chen, T., Zou, X., Zhu, M., Chen, D., & Pan, M. (2017). The adsorption of Cd(II) on manganese oxide investigated by batch and modeling techniques. *International Journal of Environmental Research and Public Health 14*. https://doi.org/10.3390/ijerph14101145

Ibisi, N., & Asoluka, C. (2018). Use of agro-waste (Musa paradisiaca peels) as a sustainable biosorbent for toxic metal ions removal from contaminated water. *Chemistry International 4*, 52-59. Retrieved from http://bosaljournals.com/chemint/images/pdffiles/18-7.pdf

Joshi, N. C., Singh, A., & Rajput, H. (2018). Utilization of waste leaves biomass of myrica esculenta for the removal of Pb(II), Cd(II) and Zn(II) ions from waste waters. *Oriental Journal of Chemistry 34*, 2548-2553. https://doi.org/10.13005/ojc/340542

Kan, T., Strezov, V., & Evans, T. J. (2016). Lignocellulosic biomass pyrolysis: A review of product properties and effects of pyrolysis parameters. *Renewable and Sustainable Energy Reviews 57*, 1126-1140. https://doi.org/10.1016/j.rser.2015.12.185

Kaur, M., Kumari, S., & Sharma, P. (2020). Removal of Pb (II) from aqueous solution using nanoadsorbent of *Oryza sativa* husk: Isotherm, kinetic and thermodynamic studies. *Biotechnology Reports 25*, e00410. https://doi.org/10.1016/j.btre.2019.e00410

Kebede, T. G., Dube, S., Mhuka, V., & Nindi, M. M. (2019). Bioremediation of Cd(II), Pb(II) and Cu(II) from industrial effluents by *Moringa stenopetala* seed husk. *Journal of Environmental Science and Health - Part A Toxic/Hazardous Substances and Environmental Engineering 54*, 337-351. https://doi.org/10.1080/10934529.2018.1551648

Mahdi, Z., Yu, Q. J., & El Hanandeh, A. (2019). Competitive adsorption of heavy metal ions (Pb^{2+}, Cu^{2+}, and Ni^{2+}) onto date seed biochar: batch and fixed bed experiments. *Separation Science and Technology (Philadelphia) 54*, 888-901. https://doi.org/10.1080/01496395.2018.1523192

Malik, R., Dahiya, S., & lata, S. (2017). An experimental and quantum chemical study of removal of utmostly quantified heavy metals in wastewater using coconut husk: A novel approach to mechanism. *International Journal of Biological Macromolecules 98*, 139-149. https://doi.org/10.1016/j.ijbiomac.2017.01.100

Manirethan, V., Gupta, N., Balakrishnan, R. M., & Raval, K. (2019). Batch and continuous studies on the removal of heavy metals from aqueous solution using biosynthesised melanin-coated PVDF membranes. *Environmental Science and Pollution Research*, 1-15. https://doi.org/10.1007/s11356-019-06310-8

Medellin-Castillo, N. (2017). Bioadsorción de plomo (II) presente en solución acuosa sobre residuos de fibras naturales procedentes de la industria ixtlera (*Agave lechuguilla* Torr. y *Yucca carnerosana* (TREL.) MCKELVEY). *Revista Internacional de Contaminación Ambiental 33*, 269-280.

Morosanu, I., Teodosiu, C., Paduraru, C., Ibanescu, D., & Tofan, L. (2017). Biosorption of lead ions from aqueous effluents by rapeseed biomass. *New Biotechnology 39*, 110-124. https://doi.org/10.1016/j.nbt.2016.08.002

Obike, A. I., Igwe, J. C., Emeruwa, C. N., & Uwakwe, K. J. (2018). Equilibrium and kinetic studies of Cu (II), Cd (II), Pb (II) and Fe (II) adsorption from aqueous solution using cocoa (*Theobroma cacao*) pod husk. *Journal of Applied Sciences and Environmental Management 22*, 182-190.

Osińska, M. (2017). Removal of lead(II), copper(II), cobalt(II) and nickel(II) ions from aqueous solutions using carbon gels. *Journal of Sol-Gel Science and Technology 81*, 678-692. https://doi.org/10.1007/s10971-016-4256-0

Pan, H., Geng, Y., Dong, H., Ali, M., & Xiao, S. (2019). Sustainability evaluation of secondary lead production from spent lead acid batteries recycling. *Resources, Conservation and Recycling 140*, 13-22. https://doi.org/10.1016/j.resconrec.2018.09.012

Peng, S. H., Wang, R., Yang, L. Z., He, L., He, X., & Liu, X. (2018). Biosorption of

copper, zinc, cadmium and chromium ions from aqueous solution by natural foxtail millet shell. *Ecotoxicology and Environmental Safety 165*, 61-69. https://doi.org/10.1016/j.ecoenv.2018.08.084

Qiu, H., Lv, L., Pan, B. C., Zhang, Q. J., Zhang, W. M., & Zhang, Q. X. (2009). Critical review in adsorption kinetic models. *Journal of Zhejiang University: Science A 10*, 716-724. https://doi.org/10.1631/jzus.A0820524

Raikar, R. V., Correa, S., & Ghorpade, P. (2015). Removal of lead (II) from aqueous solution using natural and activated rice husk. *International Research Journal of Engineering and Technology (IRJET), 2*, 1677-1686.

Rasmey, A.-H. M., Aboseidah, A. A., & Youssef, A. K. (2018). Application of Langmuir and Freundlich isotherm models on biosorption of Pb^{2+} by freez-dried biomass of *Pseudomonas aeruginosa. Egyptian Journal of Microbiology 53*, 37-48. https://doi.org/10.21608/ejm.2018.2998.1050

Rinaldi, R., Yasdi, Y., & Hutagalung, W. L. C. (2018). Removal of Ni (II) and Cu (II) ions from aqueous solution using rambutan fruit peels (*Nephelium lappaceum* L.) as adsorbent. *AIP Conference Proceedings 2026*. https://doi.org/10.1063/1.5065058

Saad, A. A., Amer, R. A., Tayeb, E. H., Nady, N., & Mohamed, R. G. (2020). Unmodified rice straw for the lead removal approach from synthetic lead solution. *Alexandria Science Exchange Journal 41*, 43-52. https://doi.org/10.21608/asejaiqjsae.2020.74227

Saravanan, A., Kumar, P. S., Carolin, C. F., & Sivanesan, S. (2017). Enhanced adsorption capacity of biomass through ultrasonication for the removal of toxic cadmium ions from aquatic system: Temperature influence on isotherms and kinetics. *Journal of Hazardous, Toxic, and Radioactive Waste 21*, 1-24. https://doi.org/10.1061/(ASCE)HZ.2153-5515.0000355

Silas, T. V. (2017). Characterization and adsorption isotherm studies of Cd (II) And Pb (II) ions bioremediation from aqueous solution using unmodified sorghum husk. *Journal of Applied Biotechnology & Bioengineering 2*. https://doi.org/10.15406/jabb.2017.02.00034

Singh, Y. D., Mahanta, P., & Bora, U. (2017). Comprehensive characterization of lignocellulosic biomass through proximate, ultimate and compositional analysis for bioenergy production. *Renewable Energy 103*, 490-500. https://doi.org/10.1016/j.renene.2016.11.039

Taşar, Ş., Kaya, F., & Ozer, A. (2014). Biosorption of lead (II) ions from aqueous solution by peanut shells: Equilibrium, thermodynamic and kinetic studies. *Journal of Environmental Chemical Engineering 2*, 1018-1026. https://doi.org/10.1016/j.jece.2014.03.015

Tejada-Tovar, Candelaria;, Bonilla-Mancilla, H., Del Pino-Moreyra, J., Ortega-Toro, R., & Villabona-Ortíz, A. (2020). Effect of the adsorbent dose in Pb(II) removal by using sugar cane bagasse: Kinetics and isotherms. *Revista Mexicana de Ingeniería Química 12*, 505-511. Retrieved from http://www.redalyc.org/articulo.oa?id=62029966013

Tejada-Tovar, Candelaria;, Herrera-Barros, A., & Ruiz-Paternina, E. (2016). Utilización de biosorbentes para la remoción de níquel y plomo en sistemas binarios. *Ciencia En Desarrollo 7*, 31-36. https://doi.org/10.19053/01217488.4228

Tejada-Tovar, Candelaria, Gonzalez-Delgado, A., & Villabona-Ortiz, A. (2019). Characterization of residual biomasses and its application for the removal of lead ions from aqueous solution. *Applied Sciences 9*, 4486. https://doi.org/10.3390/app9214486

Tran, H. N., Nguyen, D. T., Le, G. T., Tomul, F., Lima, E. C., Woo, S. H., ...Chao, H. P. (2019). Adsorption mechanism of hexavalent chromium onto layered double hydroxides-based adsorbents: A systematic in-depth review. *Journal of Hazardous Materials 373*, 258-270. https://doi.org/10.1016/j.jhazmat.2019.03.018

ul Haq, A., Saeed, M., Anjum, S., Bokhari, T. H., Usman, M., & Tubbsum, S. (2017). Evaluation of sorption mechanism of Pb (II) and Ni (II) onto Pea (*Pisum sativum*) peels. *Journal of Oleo*

Science 743, 735-743. https://doi.org/10.5650/jos.ess17020

Villabona-Ortíz, A., Tejada-Tovar, C., & Ortega-Toro, R. (2020). Modelling of the adsorption kinetics of Chromium (VI) using waste biomaterials. *Revista Mexicana de Ingeniería Química 19*, 401-408. https://doi.org/10.24275/rmiq/IA650

Yu, X. L., & He, Y. (2018). Optimal ranges of variables for an effective adsorption of lead(II) by the agricultural waste pomelo (*Citrus grandis*) peels using Doehlert designs. *Scientific Reports 8*, 1-9. https://doi.org/10.1038/s41598-018-19227-y

Zhou, N., Chen, H., Xi, J., Yao, D., Zhou, Z., Tian, Y., & Lu, X. (2017). Biochars with excellent Pb(II) adsorption property produced from fresh and dehydrated banana peels via hydrothermal carbonization. *Bioresource Technology 232*, 204-210. https://doi.org/10.1016/j.biortech.2017.01.074